IADC/SPE-212503-MS

Automatic Classification of PDC Cutter Damage Using a Single Deep Learning Neural Network Model

Abdulbaset Ali, Memorial University of Newfoundland, College of Electronic Technology-Tripoli; Harnoor Singh and Daniel Kelly, Memorial University of Newfoundland; Donald Hender, IPCOS, Memorial University of Newfoundland; Alan Clarke, ACBBtech; Mohammad Mahdi Ghiasi, Ronald Haynes, and Lesley James, Memorial University of Newfoundland

This paper was prepared for presentation at the IADC/SPE International Drilling Conference and Exhibition, Stavanger, Norway, 7 – 9 March 2023.

Abstract

There is considerable value in automatically quantifying cutter damage from drill bit pictures. Current approaches do not classify cutter damage by type, i.e., broken, chipped, lost, etc. We, therefore, present a computer vision model using deep learning neural networks to automate multi-type damage detection in Polycrystalline Diamond Compact (PDC) drill bit cutters.

The automated bit damage detection approach presented in this paper is based on training a computer vision model on different cutter damage types aimed at detecting and classifying damaged cutters directly. Prior approaches detected cutters first and then classified the damage type for the detected cutters. The You Only Look Once version 5 (YOLOv5) algorithm was selected based on the findings of an earlier published study. Different models of YOLOv5 were trained with different architecture sizes with various optimizers using two-dimensional (2D) drill bit images provided by the SPE Drilling Uncertainty Prediction technical section (DUPTS) and labeled by the authors with training from industry subject matter experts. To achieve the modeling goal, the images were first annotated and labeled to create training, validation, and testing sub-datasets. Then, by changing brightness and color, the images allocated for the training phase were augmented to generate more samples for the model development. The categories defined for labeling the DUPTS dataset were bond failure, broken cutter, chipped cutter, lost cutter, worn cutter, green cutter, green gauge, core out, junk damage, ring out, and top view. These categories can be updated once the IADC upgrade committee finishes upgrading IADC dull bit grading cones.

Trained models were validated using the validation dataset of 2D images. It showed that the large YOLOv5 with stochastic gradient descent (SGD) optimizer achieved the highest metrics with a short training cycle compared to the Adam optimizer. In addition, the model was tested using an unseen data set collected from the local office of a drill bit supplier. Testing results illustrated a high level of performance. However, it was observed that inconsistency and quality of rig site drill bit photos reduce model accuracy. Therefore, it is suggested that companies produce large sets of quality images for developing better models. This study successfully demonstrates the integration of computer vision and machine learning for drill bit

grading by categorizing/classifying damaged cutters by type directly in one stage rather than detecting the cutters first and then classifying them in a second stage. To guarantee the deployed model's robustness and consistency the model deployment has been tested in different environments that include cloud platform, container on a local machine, and cloud platform as a service (PaaS) with an online web app. In addition, the model can detect ring out and cored damages from the top view drill bit images, and to the best of the authors' knowledge, this has not been addressed by any study before.

The novelty of the developed deep learning computer vision algorithm is the ability to detect different cutter damage types in a fast and efficient process compared to the current lengthy manual damage evaluation practice. Furthermore, the trained model can detect damages that frequently take place in more than one blade of the bit such as ring outs and coring. In addition, a user-friendly interface was developed that generates results in pdf and CSV file formats for further data analysis, visualization, and documentation. Also, all the technologies used in the development of the model are open source and we made our web app implementation open access.

Introduction

The drill bit is an integral component of any drill string design. It must withstand energy generated by the drilling system to penetrate subsurface rock during the well construction process. The condition of the drill bit is a good indicator of what happened downhole and is a critical factor impacting drilling efficiency and performance. Furthermore, forensics analysis of the bit condition can help determine changes in operating parameters to enhance bit performance and longevity, encourage drill bit vendors to re-engineer solutions for future drilling bit runs, save time, and reduce drilling exposure at the rig site.

Traditionally, operational teams manually perform onsite visual inspections of drill bits to assess post-run damage conditions using a set of IADC (International Association of Drilling Contractors) grading guidelines that were developed in 1987 (Clark et al. 1987; Winters and Doiron 1987) and were last revised in 1992 (Brandon et al. 1992). However, this process is highly dependent on human perception making it prone to subjectivity. Nowadays, mobile cameras, image processing, and advanced object detection algorithms can now be leveraged for computer automation of blade-wise PDC cutter damage identification, transforming dull bit evaluation into a more reliable and objective process (Ashok et al. 2020; Gjertsen et al. 2023). Furthermore, new standardized documentation practices (Watson et al. 2022) provide guidelines for capturing photos at the rig site, and therefore the quality of images is expected to improve significantly over time. This increases the viability of having a software driven application to assess bit condition onsite to support real-time rig decisions, and in the lab to accelerate detailed forensics. Consistent and accurate bit damage identification is key to unlocking advanced bit forensics (Pastusek et al. 2022; Witt-Doerring et al. 2021). Previous attempts to automate the dull bit grading process by using photos of drill bits (Ashok et al. 2020; Lu et al. 2022) did not classify the type of damage to the cutters in drill bits. This investigation suggests a way to detect the cutters and classify the type of cutter damage with a single object detection model.

Literature Review

There have been attempts to automate the dull bit grading process by using photos of drill bits taken at the rig site. Ashok et al. (2020) compared several object detection models to identify cutters using existing drill bit photos and synthesized images of drill bits using a Computer-Aided Design (CAD) model. They concluded that the YOLOv3 model, a type of Convolutional Neural Network (CNN), performed to a high degree of accuracy for cutter detection among the available object detection models tested in their investigation. Mean Average Precision (mAP) and Frame Per Second (FPS) were performance metrics chosen for their evaluation. Image processing techniques were used to quantify the cutter damage and a degree of wear was assigned according to the 1987's IADC dull grading standard. Some of these methods were available as built-in functions in OpenCV, an image processing library in several programming languages.

Ashok et al. (2021) proposed a solution to identify the root cause of bit damage and failure. This was achieved by extending the cutter image methodology presented by Ashok et al. (2020). The new approach by Ashok et al. (2021) includes two additional steps as follows:

1. Use a cutter localization algorithm designed to identify the focal blade and group its cutters into regions (nose, shoulder, cone, and gauge).
2. Use a decision tree classifier model to use the average damage that occurred in various parts of the blades to infer root cause of damage.

The authors first identified the focal blade of interest in input images to avoid overcounting cutters that are in the background of an image. Then, they proposed to zone the focal blade into cone, nose, shoulder, and gauge, since damage in different regions of a blade indicates different possible causes. This was achieved by using the angles between the slopes joining the center points of cutters on the focal blade. After that, they trained a simple decision tree model to predict the cause of the damage. A dataset of wells which included multiple bit images, surface sensor data, downhole vibration data, and offset well rock strength information was available to help relate the type of drilling dysfunction to regions of quantified damage. One important observation was found that the accuracy of both cutter detection and damage quantification significantly improved with good lighting and resolution. This requires a minimalistic infrastructure (photo capture using a mobile phone and image storage) which is practical for rig site evaluation, although when bit images are not captured appropriately, the accuracy of this method will decrease.

Lu et al. (2022) compared object detection algorithms to detect the bit, blades, and cutters. They found that YOLOv3 was faster and more accurate than Faster R-CNN to detect each component in images where every part (bit, blades, and cutters) was present. However, Faster R-CNN was more accurate if only cutters were present. Lu et al. (2022) also generated 3D structures of drill bits using multi-view reconstruction. They then used Pointnet++ and RandLA-Net for 3D segmentation. This further improved the accuracy of object detection. However, they found that newer models took a lot longer to train and run and showed no significant detection accuracy improvement compared to YOLOv3 and Faster RCNN in images with complex lighting.

Alalsayednassir et. al. (2022) describes a more advanced system that involves scanning a physical drill bit to auto-generate a 3D visualization, which is then digitally analyzed with a dull bit grading software to assess wear and damage, on an individual cutter basis, as well as an overall bit basis. The digital format can be used with machine learning to conduct forensic analysis and cross-referenced with drilling operating parameters to help diagnose bit damage root cause. This approach offers high resolution and metrologically accuracy to accelerate bit forensics, although the solution infrastructure requires combining advanced hardware with software technologies.

In this paper, our objective is to automate the classification of PDC cutter damage using a single step deep learning neural network model and 2D images of dull drill bits. Predicting the type of damage to cutters, which is essential in PDC bit dull grading, has not been investigated to date, though some work has been proposed for publication (Gjertsen et al. 2023). Based on the work from Ashok et al. (2020, 2021) and Lu et al. (2022), it can be concluded that YOLOv3 is the best choice in terms of speed and accuracy. Therefore, YOLOv5, the most recent YOLO algorithm at the time of the development of the computer vision model, was used in this study.

Dataset

The datasets used to train the model were provided by the Society of Petroleum Engineers – Drilling Uncertainty Prediction Technical Section (SPE-DUPTS) (Witt-Doerring et al. 2021), (Ashok et al. 2020). The dataset included 956 images for more than 120 bits provided by two companies (ExxonMobil and Apache). The images were unlabeled, so our first step was to label the images after receiving relevant

training in dull bit grading and reviewing related literature. Fig. 1 includes some example images from the dataset. As illustrated, the dataset images are not standardized as angle, resolution, and lighting vary from one-bit image set to another. A set of 138 images provided by the local office of NOV Inc., St. John's, NL was added to the dataset.

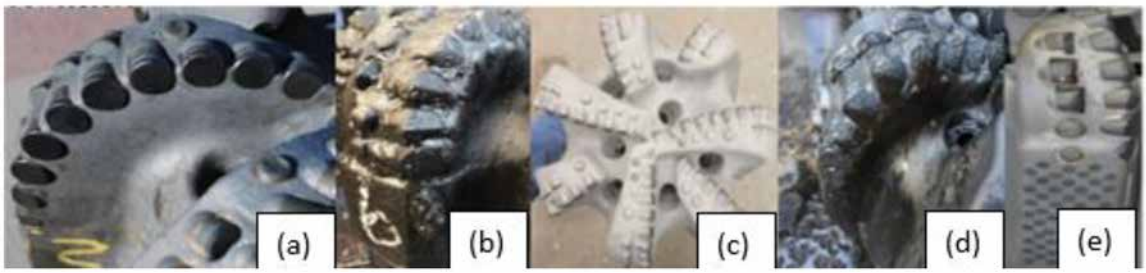

Figure 1—Sample of images from the original dataset showing; (a) Blade from top angle, (b) A different blade covered in drilling fluid from side angle, (c) Top view of a bit, (d) Another blade from side angle showing cutters, (e) 90-degree side view of a blade.

Classification of damage

Considering the damage types in the images within the provided dataset, there are eleven classes that the model can identify: bond failure, broken cutter, chipped cutter, lost cutter, worn cutter, green cutter, green gauge, core out, junk damage, ring out, and top view. These damage classifications are commonly known in the industry. Images depicting various types of damage (Figs. 2–10) were adapted from the dataset provided by SPE-DUPTS (Ashok et al. 2020; Witt-Doerring et al. 2021).

Bond Failure. Bond failure (as in Fig. 2) occurs when the polycrystalline diamond surface detaches completely from the tungsten carbide substrate in a cutter, leaving a clean surface behind. This damage is usually a manufacturing defect and/or high axial loading and is exceedingly rare to observe.

Figure 2—Example of bond failure

Broken Cutter. In a broken cutter, the cutter breaks in an irregular pattern, damaging both PDC surface and substrate. Probable causes for broken cutters include but are not limited to bit/bottom-hole-assembly whirl, downhole vibrations, high heat, interbedded hard formations, and junk damage (Pastusek et al. 2018; Dupriest et al. 2020; Pastusek 2021) (Fig. 3).

Figure 3—Example of broken cutter

Chipped Cutter. If a cutter is chipped, it exhibits sharp and irregular breaks of thin layers of the PDC layer and/or substrate in a circular or elliptical pattern, as shown in Fig. 4. Chipped cutters are usually caused by downhole vibrations or sometimes by thermal degradation. This is quite a common type of cutter damage.

Figure 4—Example of chipped cutter

Lost Cutter. A cutter is lost (as in Fig. 6) when a whole cutter (PDC layer and substrate) is totally missing from a blade, leaving a clean empty surface behind. This is usually a manufacturing/repairing issue and, therefore, very rarely observed.

Figure 5—Example of lost cutter

Figure 6—Example of worn cutter

Worn Cutter. A cutter gets worn out and exhibits normal wear. This is usually expected and is quite commonly observed, as seen in Fig. 6.

Green Cutter. A cutter is labeled a graded green cutter if it shows no wear or damage. Fig. 7 illustrates a green cutter.

Figure 7—Example of green cutter

Cored/Core Out. In a core out, as shown in Fig. 8, the center of the cutting structure of the bit is completely removed. This usually occurs due to junk or the formation being too hard.

Figure 8—Example of core out

Junk Damage. Junk damage constitutes massive amounts of damage to the cutting structure and/or the body of the bit. For cutting structure, this is identified by catastrophic damage to numerous cutters in one specific region of the cutting structure. Fig. 9 shows an example of junk damage.

Figure 9—Example of junk damage

Ring Out. In a ring out (as shown in Fig. 10), most of the cutting structure is missing in the shape of a ring (the region between two concentric circles). This usually affects all blades uniformly. This is a common type of cutting structure damage. Probable causes of ring out include vibrations, hard formation transitions, junk damage, and incorrect operating parameters (WOB, RPM, Flow, mud properties).

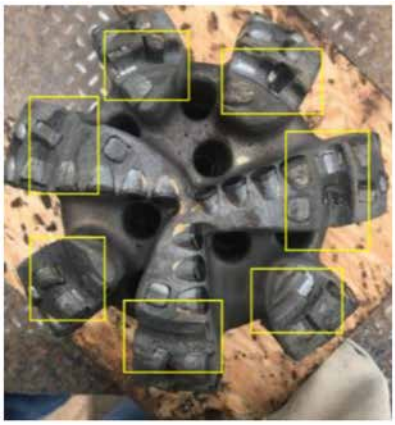

Figure 10—Example of ring out

It should be noted that there are other types of damage (balled up, erosion, heat checking, lost nozzle, plug nozzle, and wash out) that cannot be detected by the model because they were not part of the training dataset. These damage types primarily affect other parts of the bit.

Distribution of classes

After analyzing and annotating the dataset, it was observed that some damage types were more frequent in images. This is consistent with the anecdotal knowledge in the industry that drill bits suffer from some types of damage more often compared to other types. Therefore, the class distribution is uneven. Fig. 11 depicts the number of occurrences of each class in the dataset. It is clear that the distribution is imbalanced, and more 'rare' examples are currently being sought to provide a better, more balanced, training set.

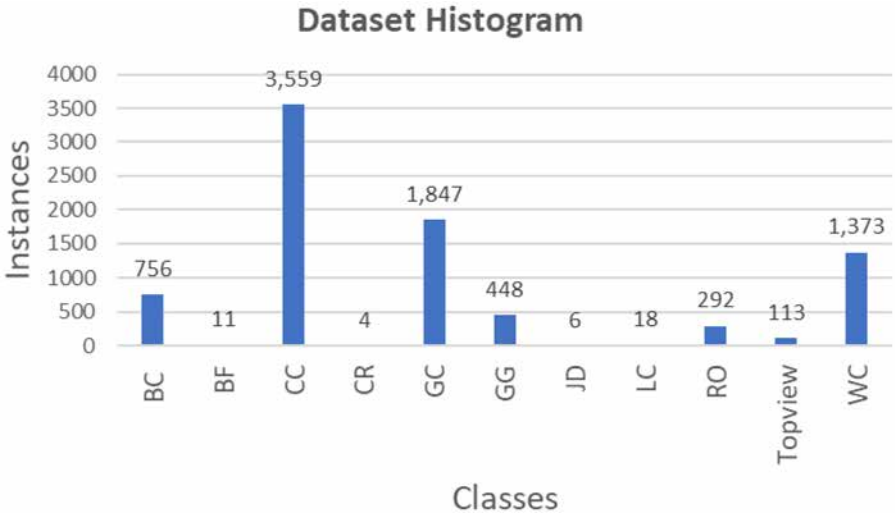

Figure 11—Number of occurrences of classes in the dataset

Methodology

The automated bit damage detection approach presented in this work is based on training a single step deep learning neural network model. The model will detect and classify PDC cutter damage types in one step using 2D images as inputs. The model capability was further enhanced to identify the focal blade and group its cutters into regions (nose, shoulder, cone, and gauge). Adding cutter localization and zones of interest to the modeling strategy will help subject matter experts link observed bit damage types with possible failure modes and accelerate bit forensics analysis (Watson et al. 2022).

Annotation and Augmentation

An online annotation tool was used for annotation. Before annotation, very low-quality images were dropped. The dataset was split into 810 images for training, 100 for validation, and 65 for testing. Furthermore, the training set was doubled via augmentation in terms of brightness (between −20% and +20%) and color (grayscale: applied to 25% of images) to generate the final dataset.

As seen in Fig. 11, some damage types are more common than others. Since most images can have more than one class/damage type, compensating by resampling underrepresented classes was not feasible without advanced image processing methods. The training and deployment workflows are illustrated in Fig. 12a and 12b respectively. Fig. 12a shows the training process starting from annotation to selecting the top-performing model using the validation set. Fig. 12b illustrates the deployment of the final selected model, where we only feed images to the damage detection model. As per Fig. 12b, the end user can choose the auto-generated output type among the following types: PDF file, CSV file, or image displayed in a browser.

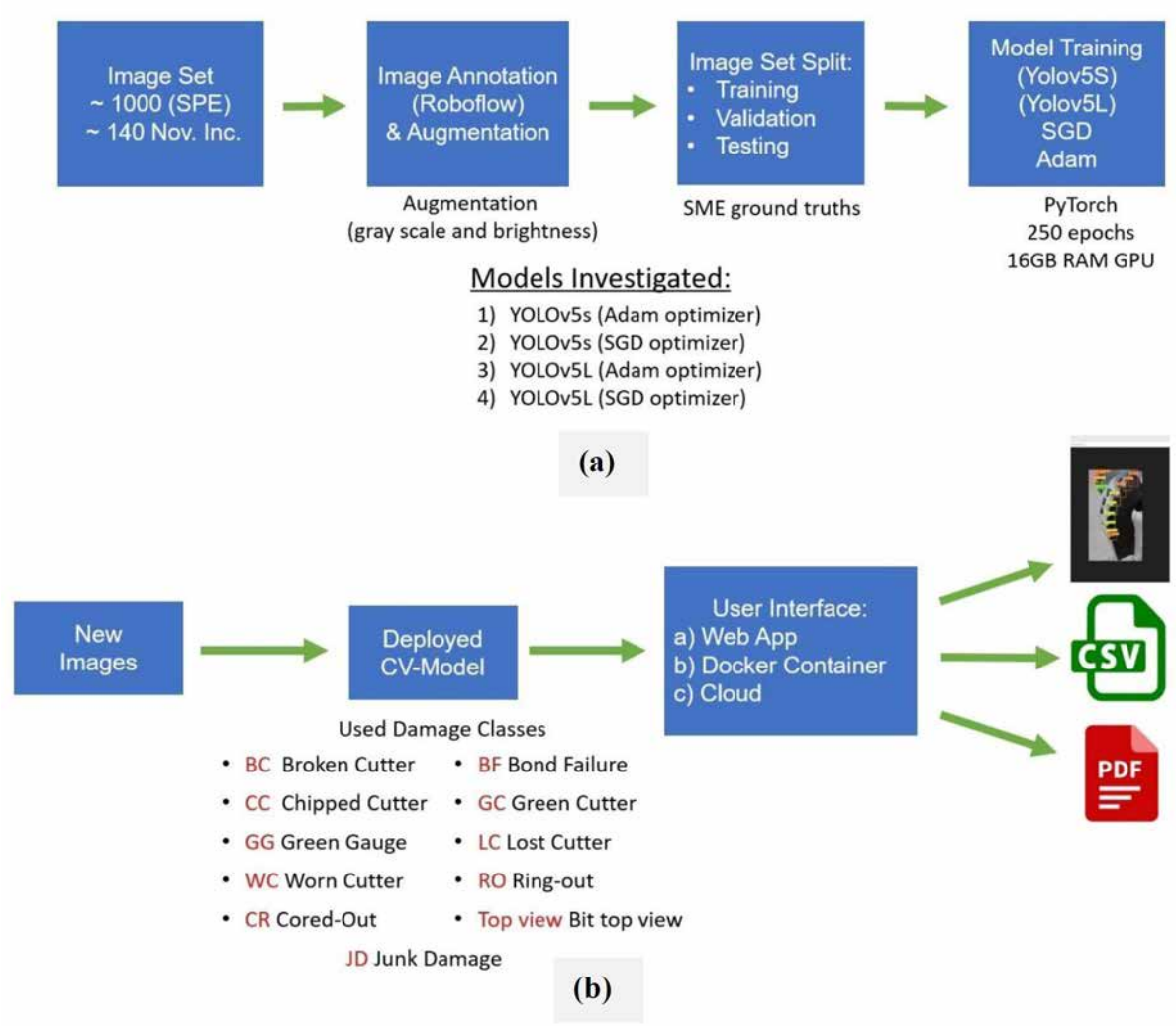

Figure 12—(a) Training cycle and (b) deployment cycle workflows

Modeling with Deep Learning & Computer Vision

Ashok et al. (2020) and Lu et al. (2022) studied the use of deep learning and computer vision for bit grading and concluded that YOLOv3 achieved a high detection accuracy rate. In our work, we started from this finding and selected YOLOv5 to detect seven cutter categories (bond failure, broken cutter, chipped cutter, lost cutter, worn cutter, green cutter, green gauge), three-bit level categories (core out, junk damage, ring out)

and a top view category. As there are different model sizes for YOLOv5 (nano, small, medium, large, and extra-large), two models were selected for training, namely YOLOv5s (small) and YOLOv5l (large). Two different optimizers, namely Adam and Stochastic Gradient Descent (SGD), were used with both small and large version for training. Thus, four models were trained in total. The reason behind choosing small YOLO architecture was to provide a fast and small-sized model suitable for web deployment. The large YOLO architecture was trained to provide a more accurate and advanced model appropriate for edge deployment with more compute resources.

Training and Validation

Model training was done using cloud computing with GPU resources. Each model was trained for 230 epochs and validated after training. Since the task is object detection, mean Average Precision (mAP@.5) is an important indicator for the model performance. Fig. 13 plots the mean Average Precision (mAP) metric for validation curves of trained models. These results show that YOLOv5 models with SGD optimizers have achieved the highest mAP@.5 values at the end of the training cycle compared to the models with Adam optimizer. It is worth mentioning that SGD models have reached 50% mAP level within the first 10 epochs. However, this was not the case for the models with the Adam optimizer, whereby it took up to 50 epochs for the small YOLOv5 and 100 epochs for the large model with the Adam optimizer. In general, the large YOLOv5 model with SGD optimizer showed a more stable mAP pattern with less fluctuation compared to the rest. In terms of the training-time small size models took about two hours each using a GPU card with 16GB RAM. On the other hand, training time for the large models with Adam and SGD optimizers was about 13 and 8 hours respectively using a 16GB RAM GPU card.

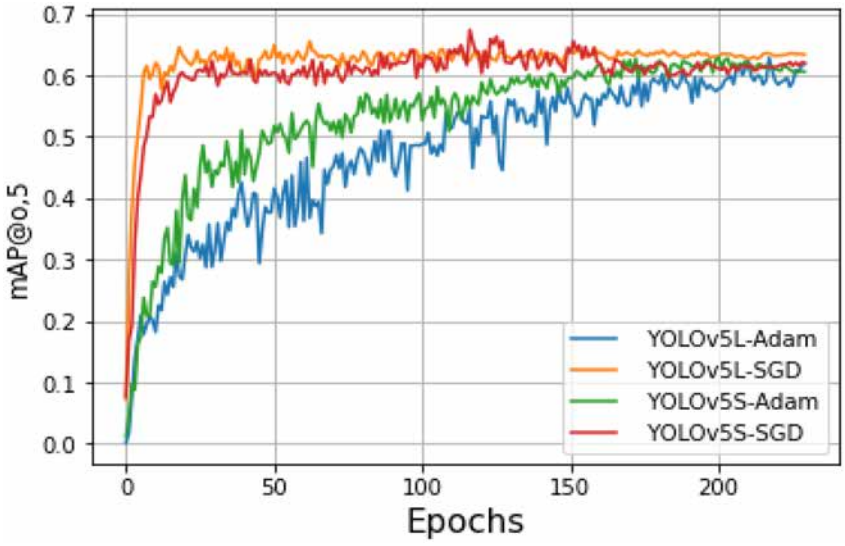

Figure 13—Validation mAP@0.5 plots for the trained models

Model Testing

For model testing, we held aside 65 images to test the four trained models. Fig. 14 depicts the number of occurrences of each class in the test set. The test was selected randomly from the original imbalanced dataset. Thus, the test set inherited the imbalance feature consequently.

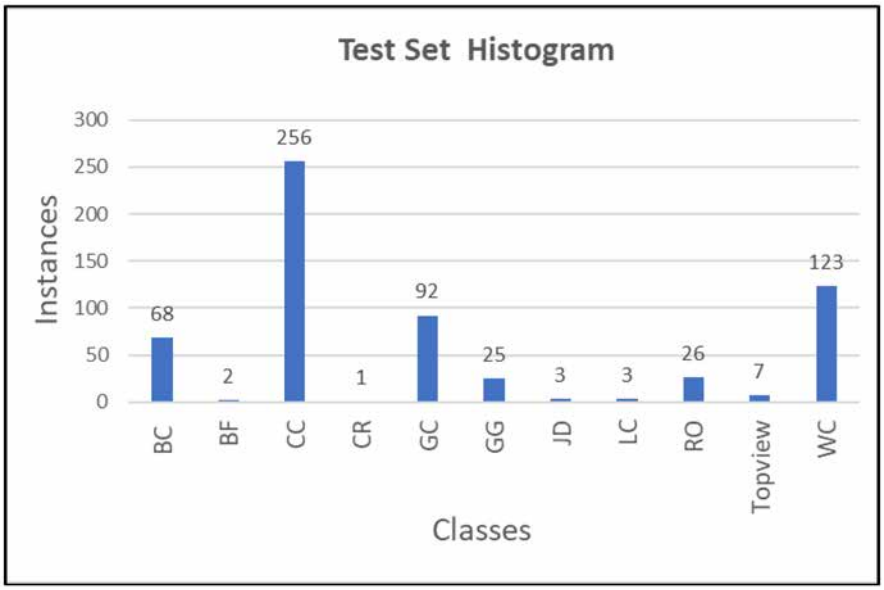

Figure 14—Number of occurrences of classes in the test set

We analyzed testing results in terms of overall performance in terms of mAP@0.5 and each class was analyzed individually using the confusion matrix. Table 1 gives the overall precision, recall, and mAP of the four trained models. Results show that both models with SGD optimizer achieved a mAP of 0.68 or higher. However, models trained with the Adam optimizer reached only 0.627 and 0.609 for large and small architectures respectively. Considering individual class results as depicted in Fig. 15 to Fig. 18, classes with good representation in the training dataset reached good classification accuracy rates. In contrast, the results for the underrepresented classes were low. For instance, bond failure was easily mixed by the models with broken, lost, or chipped cutters. In fact, the bond failure class detection rate needs to be improved by adding more images of this class to the dataset. Comparing each model performance using the confusion matrices reveals that the YOLOv5l-SGD has the highest true positive rate (the diagonal elements of the confusion matrix).

Table 1—Testing results for studied YOLO models

Model	Labels	Precision	Recall	mAP@.5
YOLOv5-large Adam	606	0.721	0.465	0.627
YOLOv5-large SGD	606	0.789	0.663	**0.689**
YOLOv5-small Adam	606	0.626	0.557	0.609
YOLOv5-small SGD	606	0.605	0.716	**0.68**

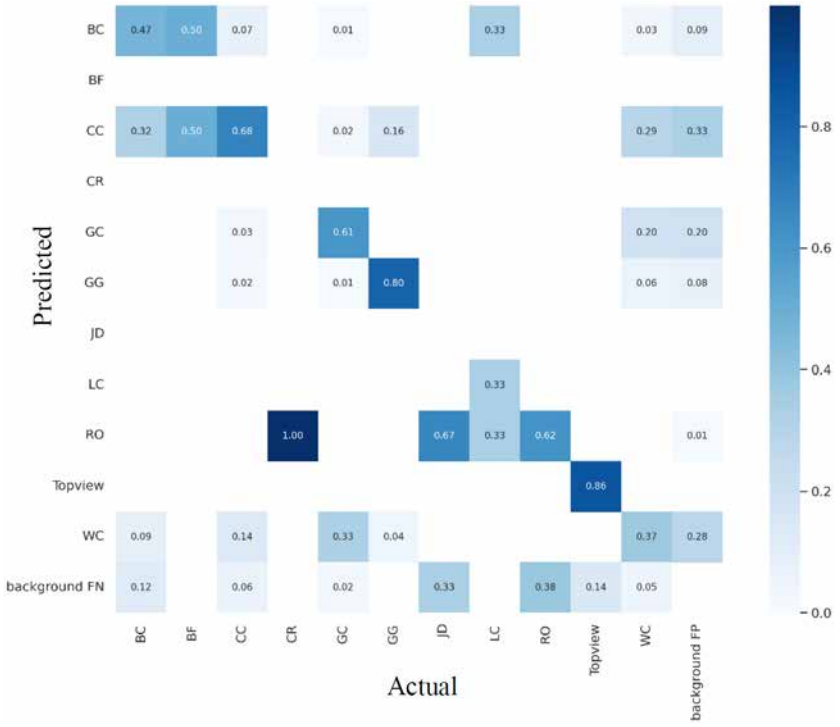

Figure 15—Confusion matrix of YOLOv5l-Amad optimizer using the test set

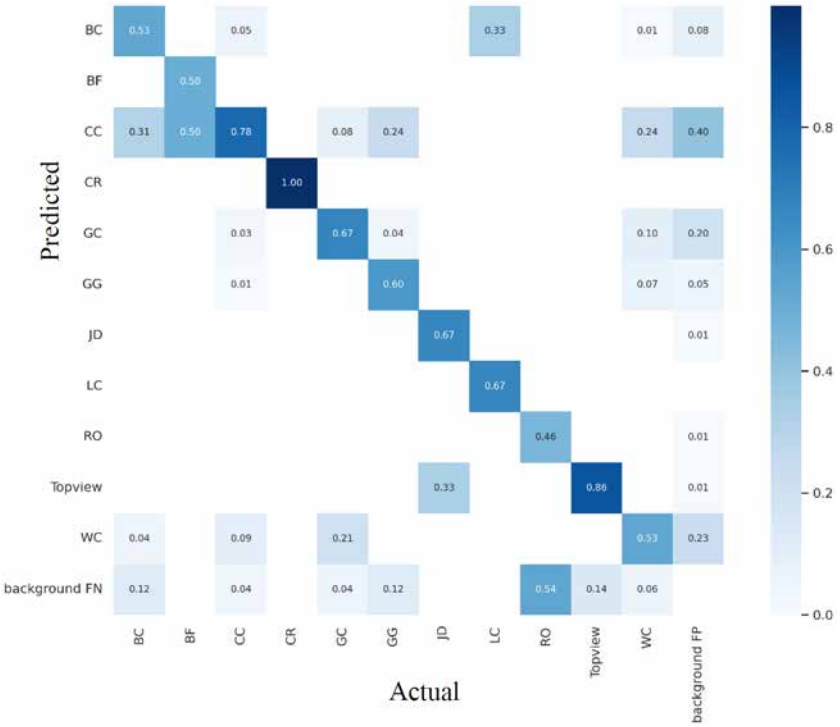

Figure 16—Confusion matrix of YOLOv5l-SGD optimizer using the test set

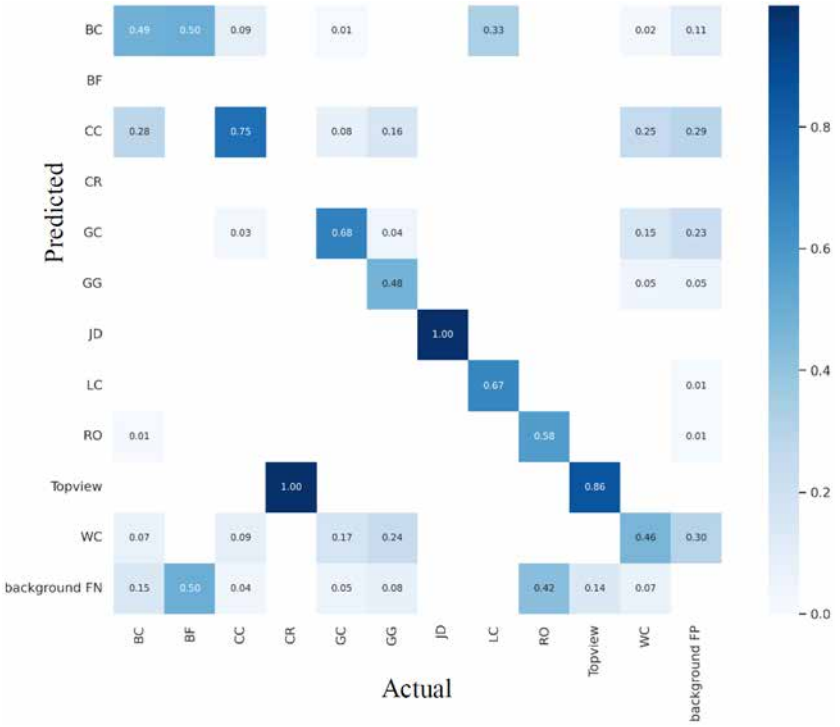

Figure 17—Confusion matrix of YOLOv5s-Amad optimizer using the test set

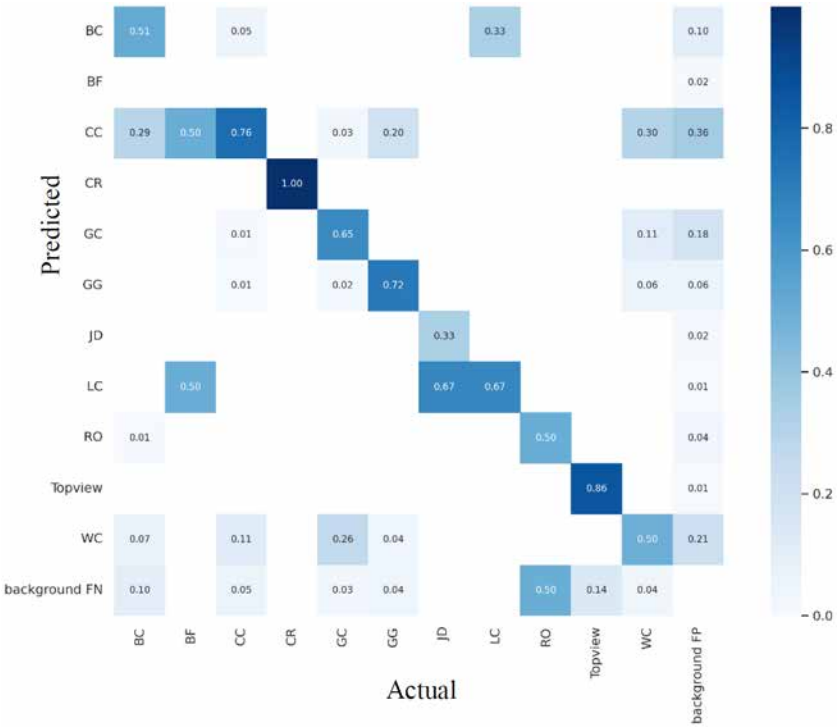

Figure 18—Confusion matrix of YOLOv5s-SGD optimizer using the test set

Discussion: Training, Validation, Testing

Training, validation, and testing results show that YOLOv5 achieved high mAP figures with a small number of training epochs. All models reached 0.5 mAP within the first 100 epochs. By comparing mAP plots, we can conclude that models using SGD optimizers outperformed the models using Adam optimizers. Models using SGD optimizer can reach 0.5 mAP within the first 10 epochs. For the final model selection,

we considered models with SGD optimizer. However, we selected YOLOv5s for any online deployment environment as it has a smaller size which is an important feature during any online model deployment where resources are limited. However, YOLOv5l with SGD optimizer is recommended for local, containerized, or cloud deployment as it showed outstanding performance for underrepresented classes such as lost cutter and bond failure.

Detection examples of the final selected models are depicted in Figs. 19 and 20. The number beside the class name on the bounding box is the confidence level given by the model.

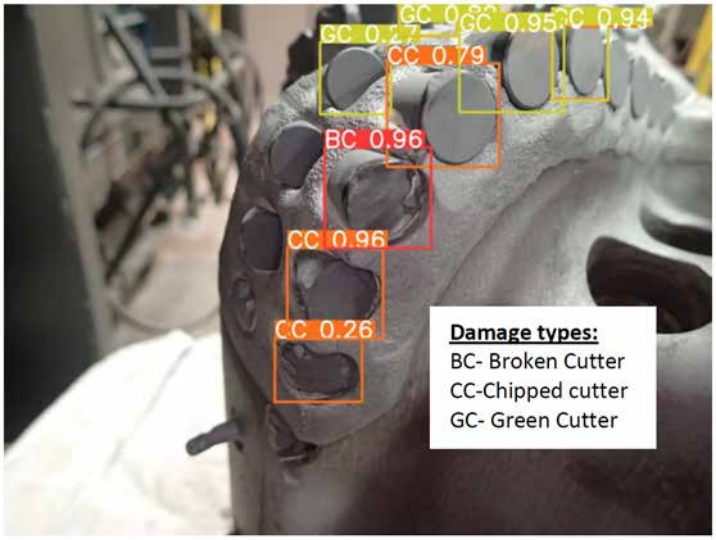

Figure 19—Model detection output on an image from the testing set – blade view

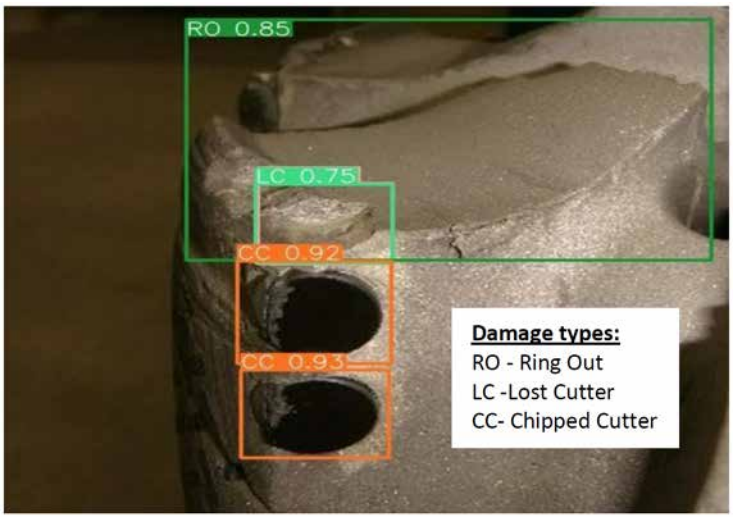

Figure 20—Model detection output on an image from the testing set – detection of ring-out on a blade

The detection results can be reported in different formats as follows:

- PDF file which shows the detection results outlined as bounding boxes for each supplied image as shown in Figs. 19 and 20 above in addition to a histogram plot showing the frequency of each damage type.
- CSV file where the results are given in a table format suitable for further data analysis.
- 2D images with bounding boxes reported back from the online web application via a browser.

Focal Blade Identification

A typical image of a blade of a drill bit usually has surrounding blades in its background. The trained model cannot distinguish between the cutters in the foreground and background, and therefore the model detects all cutters in an image. This is problematic since one cannot zone a blade into different sections without knowing how many blades there are in the image and which cutters belong to which blade. Another issue is the overcounting of the same cutters (in the background), assuming there are images of each blade present. To overcome these issues, one can just identify the blade in the forefront of an image, also called the focal blade.

To identify the focal blade, Ashok et al. (2021) used a modified version of the gift-wrapping algorithm (Jarvis 1973), which is a type of convex hull algorithm. The modification by Ashok et al. (2021) was to always start from the bottommost cutter in an image and then only go clockwise. However, this approach does not always work as intended since many edge cases were observed during the development of the software.

To further improve on the approach used by Ashok et al. (2021), the width and height of the bounding boxes of cutter detections were used as a heuristic for the algorithm. By using the width and height of the bounding boxes, the search space of the gift-wrapping algorithm was reduced to a local region near the cutter of interest in the image. This greatly increased the robustness of the algorithm. Another improvement that was implemented was to allow the model to slightly go anticlockwise given certain circumstances. This was done since it was observed that in some images, going slightly anticlockwise was required due to some images being clicked from different angles and orientations.

Results are further improved by manual (or automated) cropping of the image by the user at the beginning of the process (see Fig. 21), so that background information is removed. This also helps in handling a lot of edge cases.

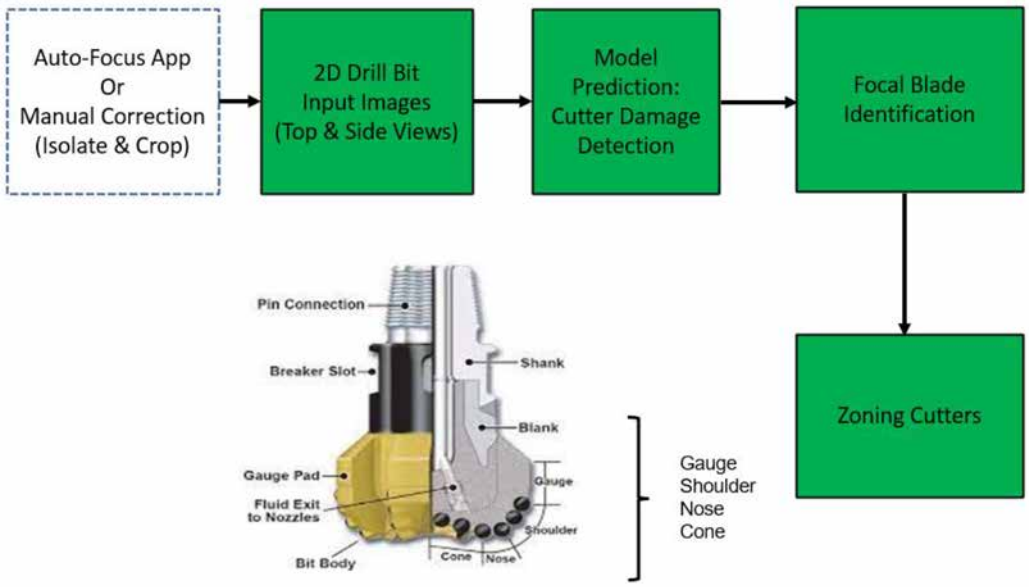

Figure 21—Methodology: Process (solid) and improvement opportunity-step (dashed) to achieve better accuracy on focal blade identification

Fig. 22 depicts an original image and a resultant image after processing the original one through the developed algorithm.

Figure 22—Detection of cutters on a focal blade from gauge up to cone.

Zoning

After identifying the focal blade, the next step is to zone the blade into different sections. There are different types of PDC drill bits, as shown in Fig. 23 (adapted from (Ashok et al. 2021)). As mentioned by Ashok et al. (2021), almost all the drill bits in the industry resemble the shape depicted in Fig. 23(d). This is also consistent with the drill bit images in the dataset. Therefore, the four sections of the blade that need to be identified are cone, nose, shoulder, and gauge.

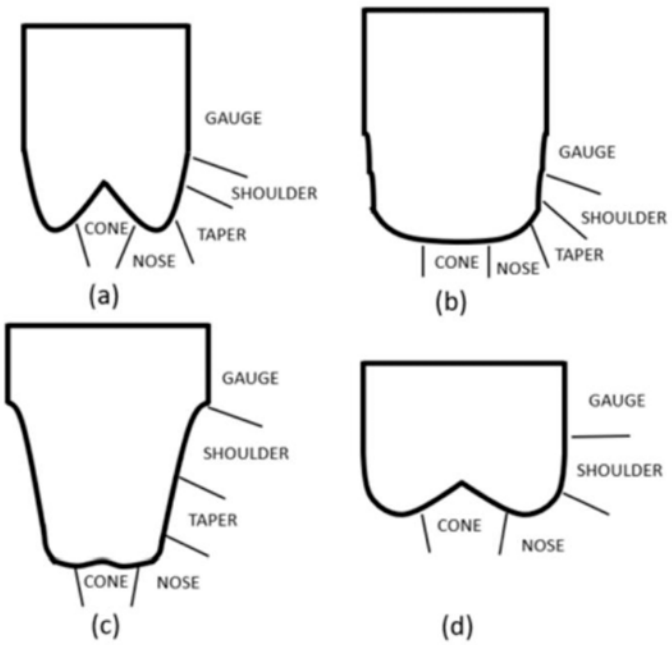

Figure 23—Cross section view of various types of PDC drill bits. Adapted from Ashok et al. (2021).

Ashok et al. (2021) used angles between the lines joining the center points of the cutter detections to classify the cutters into sections. However, it was found that this approach did not generalize well to the variety in the images. Therefore, other approaches were attempted to solve this task. The most robust algorithm among all explored options calculates discrete derivatives and double derivatives and uses this information to classify the blade into sections. Fig. 24 illustrates the output of the zoning algorithm.

Figure 24—Zoning focal blade into different sections

However, there are still limitations in the current algorithm. For instance, it is very difficult to classify gauge using differences in angles since there is negligible angle change between gauge and shoulder. Even though the gauge cutters are identified by the CV model, it cannot be relied on all the time, since it only detects undamaged gauge cutters. In cases where both shoulder and gauge cutters have similar damages, it is difficult to distinguish between them, even for humans. In such cases, the drill bit has to be compared with pre-run drill bit images to locate gauge cutters.

Determining Cause

There is considerable anecdotal knowledge amongst drilling engineers regarding the relationship between various types of damages and the causes associated with them. A few research papers also exist in the literature that explain these relationships. For instance, Pastusek et al. (2018), Dupriest et al. (2020), Pastusek (2021), Witt-Doerring (2021) and Watson et al. (2022) have explained such associations in detail.

Ashok et al. (2021) proved the concept of automated root cause determination by developing a trained decision tree model, as shown in Fig 25.

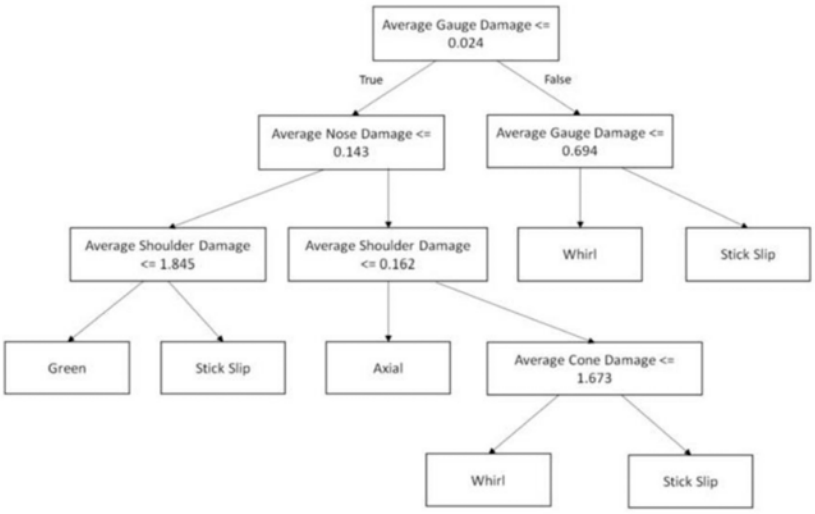

Figure 25—Sample trained decision model for forensics developed by Ashok et al. (2021)

Some pseudocode and associated flowchart were developed, which will assist the development of software that automates narrowing down of root cause determination, that the user may further investigate using drilling data. The flowchart is illustrated in Fig. 26.

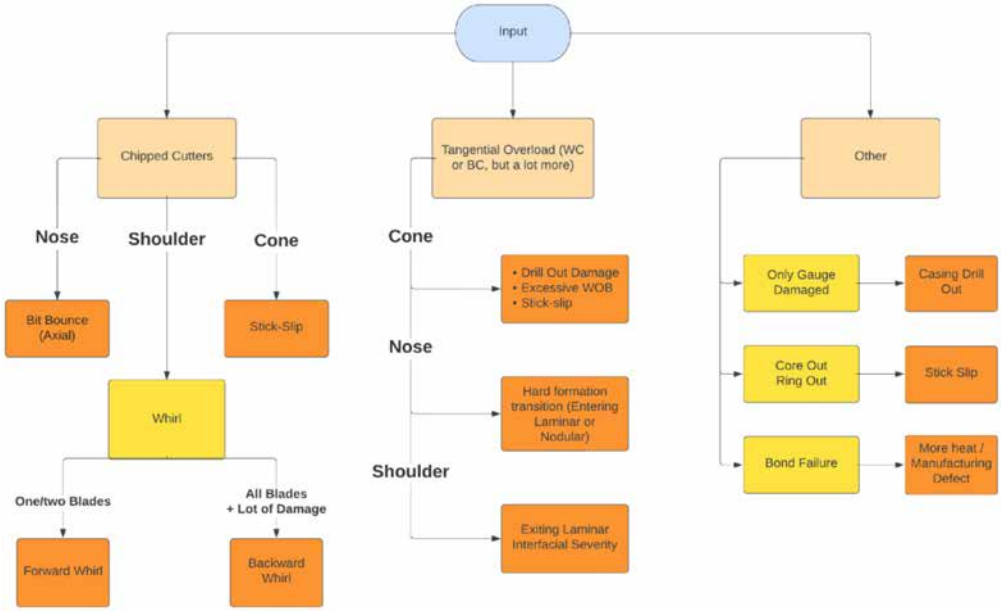

Figure 26—Proposed Flowchart for drill bit forensics

Model Deployment

Deploying the selected models in production can be implemented either remotely hosted on a cloud platform, fully implemented on a platform as a service (PaaS) with an online web application, or containerized on a local machine. Furthermore, a user interface (UI) is needed in any deployment so that the user can provide/upload bit images and receive results back.

Figs. 27 and 28 show the deployed model in action on PaaS with web app UI. At the time of writing this paper, the web app is hosted at https://drill-bit.herokuapp.com/.

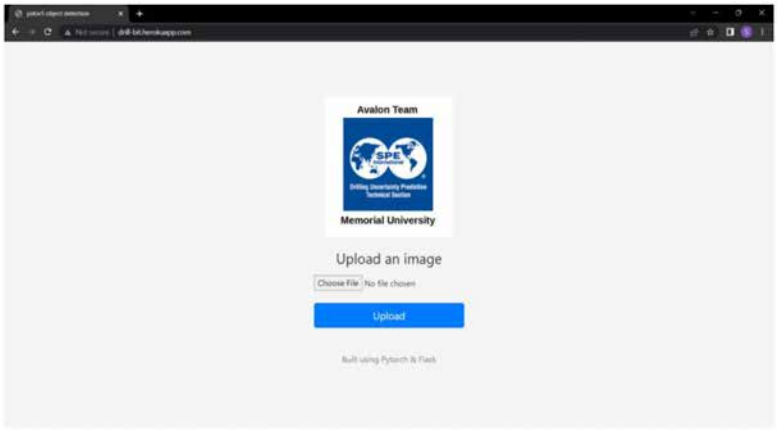

Figure 27—Landing page of deployed web app

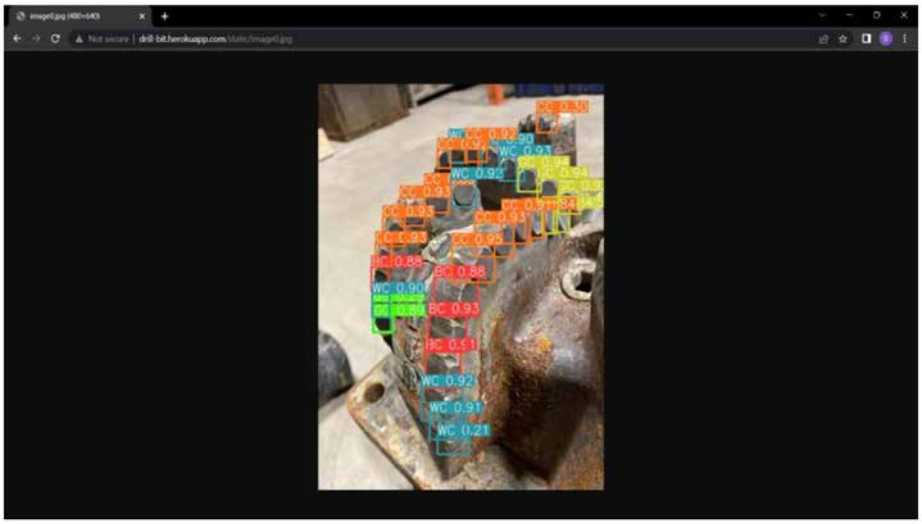

Figure 28—Output displayed by the deployed web app

Another deployment method that is being worked on at the time of the writing of this paper is a web application where subject matter experts or drilling engineers can review the results provided by the trained computer vision model and provide relevant feedback, which can be utilized to further train the model iteratively. The software has been written to standardize the structure of data obtained at various stages of the workflow in CSVs, and the same can be used to help in automating the feedback cycle. Fig. 29 shows the CSV file generated by the code for the image in Fig. 28. The 'number' column indicates the order of the primary cutters on the focused blade and the 'zone' column represents the corresponding region of interest.

id	confidence	name	fileName	number	zone
0	0.949	CC	Bit-1-27.jpg	6	S
1	0.942	GC	Bit-1-27.jpg		
2	0.94	GC	Bit-1-27.jpg		
3	0.934	CC	Bit-1-27.jpg		
4	0.933	CC	Bit-1-27.jpg	5	N
5	0.932	BC	Bit-1-27.jpg	8	S
6	0.932	CC	Bit-1-27.jpg		
7	0.931	CC	Bit-1-27.jpg		
8	0.929	WC	Bit-1-27.jpg		
9	0.923	WC	Bit-1-27.jpg		
10	0.921	WC	Bit-1-27.jpg	10	S
11	0.919	CC	Bit-1-27.jpg		
12	0.917	CC	Bit-1-27.jpg		
13	0.916	GC	Bit-1-27.jpg		
14	0.912	WC	Bit-1-27.jpg	11	S
15	0.907	BC	Bit-1-27.jpg	9	S
16	0.905	CC	Bit-1-27.jpg	4	N
17	0.895	WC	Bit-1-27.jpg		
18	0.894	CC	Bit-1-27.jpg		
19	0.888	WC	Bit-1-27.jpg		
20	0.887	BC	Bit-1-27.jpg		
21	0.885	GG	Bit-1-27.jpg		
22	0.787	WC	Bit-1-27.jpg		
23	0.784	CC	Bit-1-27.jpg	3	C
24	0.768	GC	Bit-1-27.jpg	2	C
25	0.719	WC	Bit-1-27.jpg		
26	0.714	CC	Bit-1-27.jpg		
27	0.526	WC	Bit-1-27.jpg	12	S
28	0.465	CC	Bit-1-27.jpg		
29	0.409	WC	Bit-1-27.jpg		
30	0.308	CC	Bit-1-27.jpg		
31	0.278	GC	Bit-1-27.jpg	1	C
32	0.261	BC	Bit-1-27.jpg	7	S

Figure 29—Demonstration of results in CSV format

Conclusions & Future Work

This study has successfully demonstrated the integration of CV and machine learning methods for classifying nine different rig grade classes based on IADC bit dull grading categories using the YOLOv5 algorithm and 2D images from cameras/mobile phones as inputs. It was concluded that the YOLOv5 models with SGD optimizer achieved the best mAP precision compared to models optimized with Adam. Instant damage identification using IADC dull code categories is a differentiator from previous works surveyed in the literature. Furthermore, this application can be easily integrated into the existing rig bit grading workflow to support real-time rig decisions.

Following steps can be taken in further improve the model:

- Extend damage detection to other damages such as (heat check, corrosion, erosion, etc.) by enlarging the data set with more images of these damage types.
- Package model in a smartphone application, augmented with assisted image-capturing features.
- Use surface drilling data with the CV model for drill bit forensics.
- Apply transfer learning of the current model to the new dull bit grading standard once formally published.
- Display the percentage of cutters in each category of classification

Acknowledgments

We would like to acknowledge the contributions of the SPE-DUPTS Competition 2022 Committee, Martin Lambe from NOV Inc., Ysabel Witt-Doerring from Halliburton, and Paul Pastusek and Jonathan Barry from ExxonMobil. We would also like to thank the Government of Newfoundland & Labrador, ExxonMobil, Hibernia, and Hebron partners, and the IADC Code upgrade committee for their support.

We would also like to acknowledge the usage of YOLOv5 model from Ultralytics, Roboflow, Google Colaboratory, Docker, and Flask framework as the tools used for this project.

References

Alalsayednassir, A., Berger, P., Bergfloedt, C., Schmitz, R., Schmitz, R., & Emery, S. (2022, March). AI-Enabled, Automated Digital Dull Bit Analysis - Field Experience.. International Petroleum Technology Conference. Riyadh, Saudi Arabia. doi:https://dx.doi.org/10.2523/IPTC-22001-EA

Ashok, P., Chu, J., Witt-Doerring, Y., Yan, Z., Chen, D., & van Oort, E. (2021, March). Drill bit failure forensics using 2D bit images captured at the Rig Site. SPE/IADC International Drilling Conference and Exhibition. Virtual. doi:https://doi.org/10.2118/204124-MS

Ashok, P., Vashisht, P., Kong, H., Witt-Doerring, Y., Chu, J., Yan, Z.,... Behounek, M. (2020, October). Drill Bit Damage Assessment Using Image Analysis and Deep Learning as an Alternative to Traditional IADC Dull Grading. SPE Annual Technical Conference and Exhibition. Virtual. doi:https://doi.org/10.2118/201664-MS

Brandon, B., Cerkovnik, J., Koskie, E., Bayoud, B., Clayton, R., Anderson, M.,... Niemi, R. (1992, February). First Revision to the IADC Fixed Cutter Dull Grading System. IADC/SPE Drilling Conference. New Orleans, Louisiana. doi:https://doi.org/10.2118/23939-MS

Clark, D., Coolidge, R., Kelety, J., & Kerr, J. (1987, March). Application of the New IADC Dull Grading System for Fixed Cutter Bits. SPE/IADC Drilling Conference. New Orleans, Louisiana. doi:https://doi.org/10.2118/16145-MS

Dupriest, F., Noynaert, S., Cunningham, T., & Rendon, M. (2020, March). Maximizing Drilling Performance Through the Delaware Basin Brushy Canyon and Interbedded Formations. IADC/SPE International Drilling Conference and Exhibition. Galveston, Texas. doi:https://doi.org/10.2118/199599-MS

Gjertsen, O., Leisey, J., Pastusek, P., Daechsel, D., Wolfram, P., Mushinski, R.,... Wensley, T. (2023, March). Dull Code Upgrade: Photometric Classification and Quantification of the New Dull Codes. Paper to be presented at the SPE/IADC International Drilling Conference, Stavanger, Norway. SPE-212533-MS

Jarvis, R. A. (1973, March). On the identification of the convex hull of a finite set of points in the plane. *Information Processing Letters*, **2**(1), 18-21. doi:https://doi.org/10.1016/0020-0190(73)90020-3

Lu, B., Xu, T., Huang, Y., Tao, X., Zhang, H., Yang, S.,... Wang, Z. (2022, February). Applications of Computer Vision and Deep Learning in Visual Features Extraction of Drill Bits. International Petroleum Technology Conference. Riyadh, Saudi Arabia. doi:https://doi.org/10.2523/IPTC-22624-MS

Pastusek, P., IADC Virtual Panel Discussion, 2021, April 12, *Limiter Redesign Process – Bit and BHA Forensics*. https://www.drillingcontractor.org/wp-content/uploads/2021/04/ExxonMobil-Bit-and-BHA-Forensics-TO-POST.pdf

Pastusek, P., Sanderson, D., Minkevicius, A., Blakeman, Z., & Bailey, J. (2018, March). Drilling Interbedded and Hard Formations with PDC Bits Considering Structural Integrity Limits. IADC/SPE Drilling Conference and Exhibition. Fort Worth, Texas. doi:https://doi.org/10.2118/189608-MS

Watson, W., Dupriest, F., Witt-Doerring, Y., Pastusek, P., Sugiura, J., Procter, R.,... Shackleton, D. (2022, March). IADC Code Upgrade: Bit and BHA Forensics Using Rig-Based Photographic Documentation Practices. IADC/SPE International Drilling Conference and Exhibition. Galveston. Texas. doi:https://doi.org/10.2118/208707-MS

Winters, W., & Doiron, H. (1987, March). The 1987 IADC Fixed Cutter Bit Classification System. SPE/IADC Drilling Conference. New Orleans, Louisiana. doi:https://doi.org/10.2118/16142-MS

Witt-Doerring, Y. (2021, May). A methodology to identify root cause of drill bit failure from surface drilling data and bit images. *Master Thesis, University of Texas at Austin*, Austin. https://repositories.lib.utexas.edu/handle/2152/94601

Witt-Doerring, Y., Pastusek, P., Ashok, P., & van Oort, E. (2021, September). Quantifying PDC Bit Wear in Real-Time and Establishing an Effective Bit Pull Criterion Using Surface Sensors. SPE Annual Technical Conference and Exhibition. Dubai, UAE. doi:https://doi.org/10.2118/205844-MS